ESAIM: M2AN 50 (2016) 921–944
DOI: 10.1051/m2an/2015058

**ESAIM: Mathematical Modelling and Numerical Analysis**
www.esaim-m2an.org

# A ROBUST DOMAIN DECOMPOSITION METHOD FOR THE HELMHOLTZ EQUATION WITH HIGH WAVE NUMBER*,**

Wenbin Chen[1], Yongxiang Liu[2] and Xuejun Xu[2,3]

**Abstract.** In this paper we present a robust Robin−Robin domain decomposition (DD) method for the Helmholtz equation with high wave number. Through choosing suitable Robin parameters on different subdomains and introducing a new relaxation parameter, we prove that the new DD method is robust, which means the convergence rate is independent of the wave number $k$ for $kh$ = constant and the mesh size $h$ for fixed $k$. To the best of our knowledge, from the theoretical point of view, this is a first attempt to design a robust DD method for the Helmholtz equation with high wave number in the literature. Numerical results which confirm our theory are given.

**Mathematics Subject Classification.** 65N55.

Received January 15, 2015. Revised July 24, 2015.
Published online May 23, 2016.

## 1. Introduction

The Helmholtz problem has many applications in acoustics, elasticity, electromagnetics, quantum mechanics and geophysics. Efficient and accurate numerical approximation of the Helmholtz equation is of fundamental importance in scientific computation. In the engineering application, a rule of thumb suggests that at least 8 points are needed per wavelength for the discrete problem. If we consider the pollution of the discretization of the Helmholtz equation, which requires $k^r h$ = constant, where $r > 1$, then it implies that the larger wave number $k$, the more points per wavelength are needed. So for high frequency problem, the discrete system is usually huge. Another difficulty is that the discrete algebraic system is highly indefinite for large $k$. Though there are many fast solvers for this equation in the literatures, such as shifted Laplacian [20], multigrid [2] and DD [9, 10, 13, 16] methods, but nowadays how to solve this problem fast and efficiently is still a challenging problem [8]. DD methods are important tools with their high parallel performance. In this paper, we shall

*Keywords and phrases.* Robin−Robin domain decomposition method, Helmholtz equation, optimal convergence rate.

* *The work of Wenbin Chen was supported by the Natural Science Foundation of China (11171077 and 11331004), Key Project National Science Foundation of China (91130004).*

** *The work of Xuejun Xu was supported by the National Basic Research Program under the Grant 2011CB30971 and National Science Foundation of China (No. 11171335, 11225107).*

[1] School of Mathematical Sciences, Fudan University, Shanghai 200437, China. wbchen@fudan.edu.cn

[2] LSEC, Academy of Mathematics and System Sciences, Chinese Academy of Sciences, P.O. Box 2719, Beijing 100190, China. yxliu@lsec.cc.ac.cn;xxj@lsec.cc.ac.cn

[3] Department of Mathematics, Tongji University, Shanghai 200092, China.

study a new type of nonoverlapping DD iterative method with Robin transmission conditions on the subdomain interfaces for the Helmholtz equation.

The Robin−Robin nonoverlapping DD method was proposed for the Poisson equation by Lions. The convergence rate was first proved to be $1-O(h)$ in [4,6,7,14], then it was improved by Gander *et al.* in [11] and also by Qin and Xu [17,18] to be $1-O(h^{\frac{1}{2}})$. Furthermore, it was proved by Xu and Qin *et al.* in [21] that the convergence rate is asymptotically sharp. Recently Chen *et al.* [3] presented a new two-parameter Robin−Robin method and they proved that the convergence rate of the DD method is optimal, which means that the convergence rate is independent of the mesh size $h$.

For the Helmholtz equation, the idea of using the Robin transmission conditions was first proposed by Despres in [5]. He employed the *zero*th order approximation of the Sommerfeld condition as the interface transmission condition and proved its convergence by energy method. Then Gander, Magoules, and Nataf improved the convergence rate by using so-called optimized Schwarz method in [13] with optimized *zero*th order and second order transmission conditions. Afterwards, the optimized two-sided Robin transmission condition for the Helmholtz equation was further introduced by Gander *et al.* in [12], where it is shown that the convergence rate of their DD method is $1-O(h^{\frac{1}{4}})$ for fixed $k$ and $1-O(k^{-\frac{1}{8}})$ for $kh=$ constant.

Following the idea of Chen, Xu and Zhang's method for the second-order elliptic problems, in this paper, we shall present a new two-parameter Robin−Robin DD method for the Helmholtz equation by differently choosing suitable Robin parameters, which are dependent of $h$ and $k$ on different subdomains. Meanwhile, a new relaxation parameter shall be introduced. Similar as in [11–13], we shall use Fourier transform to analyze our DD method. It is shown that the new DD method is optimal, which means the convergence rate is independent of $k$ for $kh=$ constant and also independent of $h$ for fixed frequency $k$. To the best of our knowledge, from the theoretical point of view, this is a first attempt to design a robust DD method for the Helmholtz equation with high wave number in the literature.

The outline of this paper is as follows: in Section 2, we shall present the model problem and our Robin−Robin DD method. In Section 3, we shall analyze the convergence rate of this DD method. Numerical implementation shall be given in Sections 4. Extension to many subdomains case is given in Section 5. Finally in Section 6, we present the numerical results which confirm our theory. It is seen from our numerical results that the new DD method is better than optimized Schwarz and FETI-H methods.

## 2. Model problem and DD algorithm

The model problem is as follows:

$$-\triangle u - k^2 u = f \quad \text{in } \Omega, \tag{2.1}$$

where the domain $\Omega=\mathbb{R}^2$. The Sommerfeld radiation condition at infinity with $r=(x^2+y^2)^{1/2}$ can be expressed as:

$$\lim_{r\to\infty} r^{1/2}\left(\frac{\partial u}{\partial r}-iku\right)=0, \tag{2.2}$$

which is the boundary condition for the Helmholtz equation excluding the incoming wave. In this paper, $i=\sqrt{-1}$ is the imaginary unit.

However, for practical computation, we consider the problem on a bounded region $\widetilde{\Omega}$ with some absorbing boundary condition, which actually approximates the Sommerfeld radiation condition. A usual one is the *zero*th order approximation $\frac{\partial u}{\partial n}-iku=0$ on the boundary, where $n$ is an outward normal vector at the boundary. With this condition, the variational form of the above model problem is to find $u\in V=H^1(\widetilde{\Omega})$ such that

$$(\nabla u,\nabla v)_{\widetilde{\Omega}}-k^2(u,v)_{\widetilde{\Omega}}-ik\langle u,v\rangle_{\partial\widetilde{\Omega}}=(f,v)\quad \forall v\in V,$$

where $(u,v)_{\widetilde{\Omega}}:=\int_{\widetilde{\Omega}}u\overline{v}$, $\langle u,v\rangle_{\partial\widetilde{\Omega}}:=\int_{\partial\widetilde{\Omega}}u\overline{v}$ and $\overline{v}$ is the conjugated form of $v$. This variational form has a unique solution when $f\in L^2(\widetilde{\Omega})$. If there is a piece of boundary $\widetilde{\Gamma}_r$ with condition $\frac{\partial u}{\partial n}+\gamma u=g$ or $\widetilde{\Gamma}_d$ with Dirichlet

condition, and the other part of the boundary condition is $\frac{\partial u}{\partial n} - iku = 0$, it has been proved that the variational form is to find $u \in \widetilde{V} = H^1(\widetilde{\Omega}, \widetilde{\Gamma}_d)$ such that

$$(\nabla u, \nabla v)_{\widetilde{\Omega}} - k^2(u,v)_{\widetilde{\Omega}} + \gamma\langle u, v\rangle_{\widetilde{\Gamma}_r} - ik\langle u, v\rangle_{\partial\widetilde{\Omega}\setminus(\widetilde{\Gamma}_r\cup\widetilde{\Gamma}_d)} = (f, v) + \langle g, v\rangle_{\widetilde{\Gamma}_r} \quad \forall v \in \widetilde{V},$$

where $H^1(\widetilde{\Omega}, \widetilde{\Gamma}_d)$ is the subspace of $H^1(\widetilde{\Omega})$, and for $\forall w \in H^1(\widetilde{\Omega}, \widetilde{\Gamma}_d)$, the condition $\gamma_0(w)|_{\widetilde{\Gamma}_d} = 0$ holds, where $\gamma_0(w)$ is the trace of $w$. The above equation has a solution if $\mathrm{Re}(\gamma) \geqslant 0, \mathrm{Im}(\gamma) < 0$ (Thm. 3.2 in [15]). Approximating these variational forms by finite element method is popular in practical computation.

Next, we introduce our DD algorithm for the above Helmholtz equation. The domain $\Omega$ is decomposed into two nonoverlapping subdomains $\Omega_1 = (-\infty, 0) \times \mathbb{R}$ and $\Omega_2 = (0, +\infty) \times \mathbb{R}$ with the interface $x = 0$, which is denoted by $\Gamma_{12} = \partial\Omega_1 \cap \partial\Omega_2$, and $n_i$ is an outward normal vector of $\Omega_i$ at $\Gamma_{12}(i = 1 \text{ or } 2)$. Let $f_1 = f|_{\Omega_1}, f_2 = f|_{\Omega_2}$ and $\gamma_1, \gamma_2$ be two constant parameters whose values shall be determined later. Then the DD iterative procedure can be defined as follows:

1. Solve for $u_1^n$ on $\Omega_1$

$$\begin{cases} -\triangle u_1^n - k^2 u_1^n = f_1 & \text{in } \Omega_1, \\ \dfrac{\partial u_1^n}{\partial n_1} + \gamma_1 u_1^n = g_1^n & \text{on } \Gamma_{12}, \\ \lim\limits_{r\to\infty} r^{1/2}\left(\dfrac{\partial u_1^n}{\partial r} - iku_1^n\right) = 0. \end{cases} \tag{2.3}$$

2. Update the transmission condition along the interface $\Gamma_{12}$

$$g_2^n = -\frac{\partial u_1^n}{\partial n_1} + \gamma_2 u_1^n,$$

3. Solve for $u_2^n$ on $\Omega_2$

$$\begin{cases} -\triangle u_2^n - k^2 u_2^n = f_2 & \text{in } \Omega_2, \\ \dfrac{\partial u_2^n}{\partial n_2} + \gamma_2 u_2^n = g_2^n & \text{on } \Gamma_{12}, \\ \lim\limits_{r\to\infty} r^{1/2}\left(\dfrac{\partial u_2^n}{\partial r} - iku_2^n\right) = 0. \end{cases} \tag{2.4}$$

4. Update the transmission condition along the interface again

$$g_1^* = -\frac{\partial u_2^n}{\partial n_2} + \gamma_1 u_2^n.$$

5. Relax the transmission condition along the interface

$$g_1^{n+1} = \theta g_1^* + (1-\theta) g_1^n.$$

The choice of $\gamma_1, \gamma_2$ plays an important role in our algorithm. However, the key of this algorithm is the relaxation step, without which we cannot get our optimal results.

## 3. The convergence rate of the DD method

In this section, we shall give our theoretical analysis for the algorithm introduced in the previous section.

Obviously, the solution $u$ of the model problem (2.1) is a fixed point of the iterative procedure. We only need to consider the transmission of the error functions $u_1^n - u$ and $u_2^n - u$, so it suffices to assume $f = 0$ and to analyze the convergence to the zero solution. Let $f_1 = 0, f_2 = 0$ in (2.3) and (2.4). Taking Fourier transform in

$y$ direction for each iterative step, the functions $u(x,y)$ and $g(y)$ become $\widehat{u}=\widehat{u}(x,\eta)$ and $\widehat{g}=\widehat{g}(\eta)$ respectively. We obtain the following two equations:

$$-\frac{\partial^2\widehat{u}_1^n}{\partial x^2}-(k^2-\eta^2)\widehat{u}_1^n=0 \quad x<0,\eta\in\mathbb{R}, \tag{3.1}$$

$$-\frac{\partial^2\widehat{u}_2^n}{\partial x^2}-(k^2-\eta^2)\widehat{u}_2^n=0 \quad x>0,\eta\in\mathbb{R}, \tag{3.2}$$

which are ordinary differential equations with variable $x$. The conditions

$$\frac{\partial\widehat{u}_1^n}{\partial n_1}+\gamma_1\widehat{u}_1^n=\widehat{g}_1^n, \tag{3.3}$$

$$\frac{\partial\widehat{u}_2^n}{\partial n_2}+\gamma_2\widehat{u}_2^n=\widehat{g}_2^n, \tag{3.4}$$

correspond to the boundary conditions on the interface for each subdomain. The updates of the interface transmission conditions are of the new forms

$$\widehat{g}_2^n=-\frac{\partial\widehat{u}_1^n}{\partial n_1}+\gamma_2\widehat{u}_1^n, \tag{3.5}$$

$$\widehat{g}_1^*=-\frac{\partial\widehat{u}_2^n}{\partial n_2}+\gamma_1\widehat{u}_2^n, \tag{3.6}$$

$$\widehat{g}_1^{n+1}=\theta\widehat{g}_1^*+(1-\theta)\widehat{g}_1^n. \tag{3.7}$$

Since the interface is located at $x=0$, the normal derivative is in $x$ direction. All the partial differential equations are now in the form of ordinary differential equations (ODE). Next, we solve each ODE without boundary condition for fixed $\eta$. Let $\lambda$ be the solution of the characteristic equation

$$\lambda^2+(k^2-\eta^2)=0,$$

then,

$$\lambda(\eta)=\begin{cases}\sqrt{\eta^2-k^2} & \text{if } |\eta|\geqslant k,\\ -i\sqrt{k^2-\eta^2} & \text{if } |\eta|<k.\end{cases}$$

The general solutions to the ordinary differential equations (3.1) and (3.2) without boundary conditions can be written as follows:

$$\widehat{u}_1^n(x,\eta)=A_1\mathrm{e}^{\lambda(\eta)x}+B_1\mathrm{e}^{-\lambda(\eta)x}, \quad x<0,$$
$$\widehat{u}_2^n(x,\eta)=A_2\mathrm{e}^{\lambda(\eta)x}+B_2\mathrm{e}^{-\lambda(\eta)x}, \quad x>0.$$

If we consider the absorbing boundary condition which exclude the incoming wave, then the solutions can be expressed as

$$\widehat{u}_1^n(x,\eta)=\widehat{u}_1^n(0,\eta)\mathrm{e}^{\lambda(\eta)x}, \quad \text{and} \quad \widehat{u}_2^n(x,\eta)=\widehat{u}_2^n(0,\eta)\mathrm{e}^{-\lambda(\eta)x}.$$

The expression form of $\widehat{u}_1^n$ may be explained as follows: first, for the case $|\eta|>k$, $\lambda(\eta)$ is real. Noticing that $x<0$, we have $\mathrm{e}^{\lambda(\eta)x}\to 0$ as $x\to-\infty$. However, for the item $\mathrm{e}^{-\lambda(\eta)x}$, it goes to infinity as $x\to-\infty$, which is a contradiction to the meaning of the absorbing boundary condition. Second, for the case $|\eta|<k$, $\lambda(\eta)$ is a complex number. $\mathrm{e}^{\lambda(\eta)x}$ means the left going wave, and $\mathrm{e}^{-\lambda(\eta)x}$ means the right going wave, with the frequency $\sqrt{k^2-\eta^2}$. For the third case $|\eta|=k$, $\lambda(\eta)=0$ and $\mathrm{e}^{\lambda(\eta)x}=\mathrm{e}^{-\lambda(\eta)x}$, then it can be set that $B_1=0$ for the

reason that these two basis functions are the same. Based on the above observation, in any case, the term $e^{-\lambda(\eta)x}$ should not appear in the formula of the solution $\widehat{u}_1^n$, which implies $B_1 = 0$ immediately. Similarly, we have $A_2 = 0$ in the solution $\widehat{u}_2^n$.

Substituting these expressions into the interface transmission conditions (3.3), (3.5), (3.4) and (3.6), we have

$$\begin{aligned}\widehat{g}_1^n(\eta) &= (\lambda(\eta)+\gamma_1)\widehat{u}_1^n(0,\eta),\\ \widehat{g}_2^n(\eta) &= (-\lambda(\eta)+\gamma_2)\widehat{u}_1^n(0,\eta)\\ &= (\lambda(\eta)+\gamma_2)\widehat{u}_2^n(0,\eta),\\ \widehat{g}_1^*(\eta) &= (-\lambda(\eta)+\gamma_1)\widehat{u}_2^n(0,\eta).\end{aligned}$$

Combining the above equations with the relaxation step (3.7), we get the following error propagation equation

$$\widehat{g}_1^{n+1}(\eta) = [\theta\frac{-\lambda(\eta)+\gamma_1}{\lambda(\eta)+\gamma_2}\cdot\frac{-\lambda(\eta)+\gamma_2}{\lambda(\eta)+\gamma_1}+(1-\theta)]\widehat{g}_1^n(\eta). \tag{3.8}$$

Let $\gamma_1 = p_1 - q_1 i, \gamma_2 = p_2 - q_2 i$, where $p_1, q_1, p_2, q_2 > 0$. By substituting these values into (3.8), the convergence rate $\rho$ may be expressed as follows:

$$\rho = \begin{cases} (1-\theta)+\theta\dfrac{p_1-(q_1-\sqrt{k^2-\eta^2})i}{p_2-(q_2+\sqrt{k^2-\eta^2})i}\cdot\dfrac{p_2-(q_2-\sqrt{k^2-\eta^2})i}{p_1-(q_1+\sqrt{k^2-\eta^2})i} & |\eta|<k,\\ (1-\theta)+\theta\dfrac{(p_1-\sqrt{\eta^2-k^2})-q_1 i}{(p_2+\sqrt{\eta^2-k^2})-q_2 i}\cdot\dfrac{(p_2-\sqrt{\eta^2-k^2})-q_2 i}{(p_1+\sqrt{\eta^2-k^2})-q_1 i} & |\eta|\geqslant k.\end{cases}$$

Note that for the case $|\eta| = k$, the convergence rate is $|\rho| = 1$ for any $p_1, p_2, q_1, q_2$. In another word, we cannot get the convergence rate for this case. This phenomenon is also observed by Gander *etc.* in [12,13]. Similar as in [12,13], we only consider the case $|\eta| \leqslant k_-$ and $|\eta| \geqslant k_+$, where $k_- < k < k_+$ are close to $k$. For computation, suppose that the length of $\widetilde{\Omega}$ in $y$ direction is $H$, if the upper and bottom boundary is set to be the homogeneous Dirichlet boundary, then the relevant frequencies are $\eta = \frac{j\pi}{H}, j \in \mathbb{N}$, so we may choose $k_- = k - \frac{\pi}{H}, k_+ = k + \frac{\pi}{H}$ and leave only one frequency $\eta = k$ which can be treated easily by the preconditioned Krylov method [12,13]. If $k$ satisfies $\frac{j\pi}{H} < k < \frac{(j+1)\pi}{H}$, then $\eta^2 - k^2 \neq 0$, and the iterative method converges by choosing $k_- = \frac{j\pi}{H}$ and $k_+ = \frac{(j+1)\pi}{H}$. For this homogeneous Dirichlet boundary, the lowest relevant frequency is $|\eta|_{\min} = \frac{\pi}{H}$. For other boundary conditions on top and bottom, it is not easy to determine the value of $|\eta|_{\min}$, but it is always larger or equal zero.

In the continuous case, the value of $|\eta|$ can be arbitrarily large. However, for discrete problem, we find that $|\eta| \leqslant |\eta|_{\max}$, where $|\eta|_{\max} = \frac{\pi}{h}$ is the highest frequency according to the finest mesh.

According to the above discussion, $|\eta|_{\min} \leqslant |\eta| \leqslant |\eta|_{\max}$, which is useful in the analysis of the convergence rate. Let $\underline{\eta} := |\eta|_{\min}$ and $\overline{\eta} := |\eta|_{\max}$.

Let

$$\alpha = \begin{cases}\sqrt{k^2-\eta^2} & \underline{\eta} \leqslant |\eta| \leqslant k_-,\\ \sqrt{\eta^2-k^2} & k_+ \leqslant |\eta| \leqslant \overline{\eta}.\end{cases} \tag{3.9}$$

By some elementary computation, the convergence factor should be

$$\rho = (1-\theta)+\theta\frac{A_1+iB_1}{D_1}, \quad \text{if} \quad \underline{\eta} \leqslant |\eta| \leqslant k_-,$$

where the real part $A_1$, the imaginary part $B_1$ and the denominator $D_1$ are as follows:

$$\begin{aligned}A_1 &= [(p_1p_2 - q_1q_2) - \alpha^2)]^2 + (p_1q_2 + p_2q_1)^2 - [(p_1+p_2)^2 + (q_1+q_2)^2]\alpha^2,\\ B_1 &= 2[(p_1q_2+p_2q_1)(q_1+q_2) + ((p_1p_2 - q_1q_2) - \alpha^2)(p_1+p_2)]\alpha,\\ D_1 &= [(p_1p_2 - q_1q_2) - \alpha^2 - (q_1+q_2)\alpha]^2 + [(p_1q_2+p_2q_1) + (p_1+p_2)\alpha]^2.\end{aligned}$$

For the another case of $|\eta|$, a simple calculation leads to

$$\rho = (1-\theta) + \theta\frac{A_2 + iB_2}{D_2}, \quad \text{if} \quad k_+ \leqslant |\eta| \leqslant \overline{\eta},$$

where the real part $A_2$, the imaginary part $B_2$ and the denominator $D_2$ are of the forms

$$\begin{aligned}
A_2 &= [(p_1p_2 - q_1q_2) + \alpha^2)]^2 + (p_1q_2 + p_2q_1)^2 - [(p_1+p_2)^2 + (q_1+q_2)^2]\alpha^2,\\
B_2 &= 2[-(p_1q_2 + p_2q_1)(p_1+p_2) + ((p_1p_2 - q_1q_2) + \alpha^2)(q_1+q_2)]\alpha,\\
D_2 &= [(p_1p_2 - q_1q_2) + \alpha^2 + (p_1+p_2)\alpha]^2 + [(p_1q_2 + p_2q_1) + (q_1+q_2)\alpha]^2.
\end{aligned}$$

In the following, we set $p_1 = q_1, p_2 = q_2$ for simplicity and symmetry, then the expression of $\rho$ is

$$\rho = \begin{cases} (1-\theta) + \theta\dfrac{A+iB}{D}, & \text{if} \quad \underline{\eta} \leqslant |\eta| \leqslant k_-,\\ (1-\theta) + \theta\dfrac{A-iB}{D}, & \text{if} \quad k_+ \leqslant |\eta| \leqslant \overline{\eta}, \end{cases} \tag{3.10}$$

where

$$\begin{aligned}
A &= (2q_1q_2)^2 - 2(q_1+q_2)^2\alpha^2 + \alpha^4,\\
B &= 2(2q_1q_2 - \alpha^2)(q_1+q_2)\alpha,\\
D &= (2q_1q_2 + (q_1+q_2)\alpha)^2 + (q_1+q_2+\alpha)^2\alpha^2.
\end{aligned}$$

**Lemma 3.1.** *Let $d_1$, $d_2$ and $d_3$ be defined as:*

$$d_1 = \frac{2q_1q_2}{2q_1q_2 + (q_1+q_2)\alpha}, \quad d_2 = \frac{\alpha}{(q_1+q_2)+\alpha}, \quad d_3 = \frac{2q_1q_2 - \alpha^2}{2q_1q_2 + (q_1+q_2)\alpha} \tag{3.11}$$

*then the real part of $\rho$ can be bounded by*

$$1 - 2\theta + 2\theta\min\{d_1, d_2\} \leqslant \mathrm{Re}(\rho) \leqslant 1 - 2\theta + 2\theta\max\{d_1, d_2\}, \tag{3.12}$$

*and the imaginary part of $\rho$ can be bounded by*

$$|\mathrm{Im}(\rho)| \leqslant \theta|d_3|. \tag{3.13}$$

*Proof.* By careful calculation,

$$\begin{aligned}
1 + \frac{A}{D} &= \frac{2}{D}\left(2q_1q_2(2q_1q_2 + (q_1+q_2)\alpha) + (q_1+q_2+\alpha)\alpha^3\right)\\
&= \frac{2}{D}\left(d_1(2q_1q_2 + (q_1+q_2)\alpha)^2 + d_2(q_1+q_2+\alpha)^2\alpha^2\right).
\end{aligned}$$

From the definition of $D$, $1 + \frac{A}{D}$ can be bounded by

$$2\min\{d_1, d_2\} \leqslant 1 + \frac{A}{D} \leqslant 2\max\{d_1, d_2\}. \tag{3.14}$$

Note that the real part of $\rho$ can be rewritten as

$$\mathrm{Re}(\rho) = 1 - \theta + \theta\frac{A}{D} = 1 - 2\theta + \theta\left(1 + \frac{A}{D}\right), \tag{3.15}$$

then the bound (3.12) can be obtained immediately.

On the other hand, note that $D \geqslant 2(2q_1q_2 + (q_1+q_2)\alpha)(q_1+q_2+\alpha)\alpha$, then

$$\frac{(2q_1q_2+(q_1+q_2)\alpha)(q_1+q_2)\alpha}{D} \leqslant \frac{(2q_1q_2+(q_1+q_2)\alpha)(q_1+q_2)\alpha}{2(2q_1q_2+(q_1+q_2)\alpha)(q_1+q_2+\alpha)\alpha} \leqslant \frac{1}{2}.$$

So $\frac{B}{D}$ can be bounded by

$$\frac{|B|}{|D|} = \frac{|2(2q_1q_2-\alpha^2)|}{2q_1q_2+(q_1+q_2)\alpha}\frac{(2q_1q_2+(q_1+q_2)\alpha)(q_1+q_2)\alpha}{D} \leqslant \left|\frac{2d_3}{2}\right| = |d_3|.$$

Then the bound (3.13) is easily gotten since $|\mathrm{Im}(\rho)| = \theta\frac{|B|}{|D|}$. □

**Lemma 3.2.** *If $0 < \underline{\alpha} \leqslant \alpha \leqslant \overline{\alpha}$, and assume that*

$$q_1 \leqslant \frac{C_1}{2}\underline{\alpha}, \quad q_2 \geqslant \frac{1}{C_2}\overline{\alpha}, \tag{3.16}$$

*where $0 < C_j < 1 (j = 1, 2)$, then $d_1$, $d_2$ and $d_3$ in (3.11) can be bounded by*

$$\frac{q_1}{2\overline{\alpha}} < d_1 < \frac{C_1}{C_1+1}, \tag{3.17}$$

$$\frac{\underline{\alpha}}{3q_2} < d_2 \leqslant \frac{C_2}{1+C_2}, \tag{3.18}$$

$$|d_3| < \max\left\{\frac{C_1}{C_1+1}, C_2\right\}. \tag{3.19}$$

*Proof.* Since $q_1 > 0$ and $\frac{\underline{\alpha}}{2q_1} \geqslant \frac{1}{C_1}$, then the lower bound and upper bound of $d_1$ can be estimated by

$$d_1 < \frac{2q_1q_2}{2q_1q_2+q_2\alpha} = \frac{1}{1+\frac{\alpha}{2q_1}} \leqslant \frac{C_1}{1+C_1}, \quad d_1 > \frac{2}{2+2\frac{\alpha}{q_1}} > \frac{q_1}{2\alpha} \geqslant \frac{q_1}{2\overline{\alpha}}.$$

Since $\frac{q_2}{\overline{\alpha}} \geqslant \frac{1}{C_2}$ and $q_2 > \alpha > q_1$, the bound of $d_2$ can be easily obtained

$$d_2 < \frac{\alpha}{q_2+\alpha} \leqslant \frac{C_2}{C_2+1}, \quad d_2 > \frac{\alpha}{3q_2} \geqslant \frac{\underline{\alpha}}{3q_2}.$$

Finally, from the definition of $d_3$, we have

$$|d_3| < \max\left\{d_1, \frac{\alpha^2}{2q_1q_2+(q_1+q_2)\alpha}\right\} \leqslant \max\left\{d_1, \frac{\alpha}{q_2}\right\} \leqslant \max\left\{\frac{C_1}{C_1+1}, C_2\right\},$$

so the bound (3.19) is obtained. □

**Lemma 3.3.** *If $0 < \theta < 1$ and $0 < \overline{C} < 1$, then the function*

$$\zeta(\theta) = \max\left\{|1-2\theta|^2 + \theta^2\overline{C}^2, |1-2\theta+2\theta\overline{C}|^2 + \theta^2\overline{C}^2\right\} \tag{3.20}$$

*attains the minimum value $\frac{2\overline{C}^2}{(2-\overline{C})^2}$ at $\theta_0 = \frac{1}{2-\overline{C}}$.*

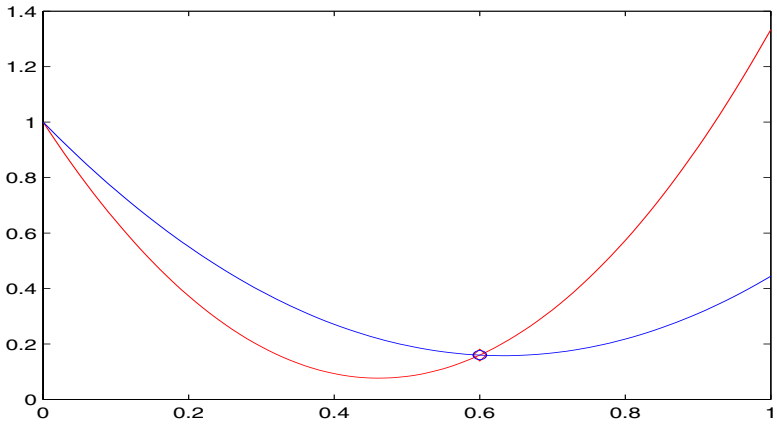


FIGURE 1. The function $\zeta(\theta)$ in (3.20) where $\overline{C} = 1/3$. The red line stands for the function $\sigma(\theta) = |1-2\theta|^2$ and the blue line stands for the function $\sigma(\theta) = |1-2\theta+2\theta\overline{C}|^2$. (Color online).

*Proof.* It is enough for us to consider the function

$$\zeta_1(\theta) = \max\{|1-2\theta|^2, |1-2\theta+2\theta\overline{C}|^2\}. \tag{3.21}$$

It is easy to be verified that (see Fig. 1)

$$\zeta_1(\theta) = \begin{cases} |1-2\theta+2\theta\overline{C}|^2, & \theta \leqslant \frac{1}{2-\overline{C}}, \\ |1-2\theta|^2, & \theta \geqslant \frac{1}{2-\overline{C}}. \end{cases}$$

When $0 < \overline{C} < 1$, the derivative of $\zeta_1$ is negative if $\theta < \frac{1}{2-\overline{C}}$ and positive if $\theta > \frac{1}{2-\overline{C}}$, therefore $\zeta_1$ attains the minimum value at $\theta_0 = \frac{1}{2-\overline{C}}$. So $\zeta(\theta)$ also attains the minimum value at $\theta_0$ and $\zeta(\theta_0) = \frac{2\overline{C}^2}{(2-\overline{C})^2}$. □

**Theorem 3.4.** *If* $0 < \underline{\alpha} \leqslant \alpha \leqslant \overline{\alpha}$, *and assume that*

$$q_1 \leqslant \frac{C_1}{2}\underline{\alpha}, \quad q_2 \geqslant \frac{1}{C_2}\overline{\alpha}, \tag{3.22}$$

*where* $0 < C_1 < 1$ *and* $0 < C_2 < \frac{2}{\sqrt{2}+1}$, *then the convergence rate* $|\rho| < 1$ *if we take* $\theta = \frac{1}{2-\overline{C}}$, *where* $\overline{C} = \max\{\frac{C_1}{C_1+1}, C_2\}$.

*Proof.* By using Lemmas 3.1 and 3.2, the real part and the imaginary part of $\rho$ can be bounded by

$$|\mathrm{Re}(\rho)| \leqslant \max\{|1-2\theta|, |1-2\theta+2\theta\overline{C}|\}, \quad \text{and} \quad |\mathrm{Im}(\rho)| \leqslant \theta\overline{C}.$$

Then following Lemma 3.3, $|\rho|$ attains the minimum value

$$|\rho| = \frac{\sqrt{2}\cdot\overline{C}}{2-\overline{C}}$$

if we set $\theta = \frac{1}{2-\overline{C}}$. Now since $0 < C_1 < 1$ and $0 < C_2 < \frac{2}{\sqrt{2}+1}$, then $\overline{C} < \frac{2}{\sqrt{2}+1}$, therefore $|\rho| < 1$. □

**Remark 3.5.** For simplicity, we shall set $\theta = \frac{1}{2}$ in the numerical tests. In this case, $|\rho|$ is still less than 1 if we require $C_2^2 < \frac{4}{5}$.

We also remark that from the definition of $\alpha$ (3.9),

$$\alpha \in [(2\tilde{C}_k k)^{\frac{1}{2}}, C_0 h^{-1}], \tag{3.23}$$

where $\tilde{C}_k = \min(k - k_-, k_+ - k)$ is a sufficient small value compared with $k$, and $C_0$ is a constant independent of $h$ and $k$. Note that $\underline{\alpha} < \overline{\eta} = \frac{\pi}{h}$, we may choose $q_2$ dependent on the mesh size $h$.

**Corollary 3.6.** *If $0 < \underline{\alpha} \leqslant \alpha \leqslant \overline{\alpha}$, and assume that*

$$q_1 \leqslant \frac{C_1}{2}\underline{\alpha}, \quad q_2 = Ch^{-1}, \tag{3.24}$$

*where $C \geqslant \frac{\pi}{C_2}$ is a constant independent of $k$ and $h$. The parameter is chosen to be $\theta = \frac{1}{2}$, then the convergence rate $|\rho| < 1$ and:*

- *is independent of $k$ for $k^r h =$ constant where $r \geqslant 1$;*
- *is independent of $h$ for fixed $k$ with $kh \leqslant$ constant.*

**Remark 3.7.** In practice, we usually choose $q_2 = C_3 h^{-m}$ with $m > 1$, where $C_3 =$ constant independent of $h$ and $k$. However, in this situation, $C_3$ is not necessarily large. We shall confirm this observation in our numerical results.

If we set at least 10 points per wavelength, by a simple calculation, $kh \leqslant \frac{\pi}{5}$, which immediately implies $\overline{\eta} \geqslant 5k$. For practical computation, to avoid the pollution error, we usually require the mesh grid $h$ to satisfy condition $k^r h =$ constant for $r \geqslant 1$. So the above result is useful.

**Remark 3.8.** The convergence result of our method is quite different from other substructuring methods, like FETI-H, FETI-DPH and BDDC-H methods. It can be seen in the above corollary that the convergent result of our DD method is independent of $h$ and $k$. For the FETI-H method, there is no any theoretical results about the convergence rate in the literature. The numerical results in [9] reveal that the iteration number increases as $k$ increasing, but it may decrease as the coarse space is sufficiently large. In [16], the convergence rate of FETI-DPH and BDDC-H is proved to be $(1 - C\frac{1}{(1+k^2H^2)(1+\log(H/h))^4})^{1/2}$ under the condition that the size of coarse grid $H$ is sufficiently small. Numerical results in [16] also shows that FETI-DPH and BDDC-H methods are scalable. However, the iteration number still increase as $k$ increasing. Meanwhile, both of these two methods also require sufficiently small $H$ to guarantee the positive definiteness of subproblem, which make the coarse space very large. So these DD methods actually cannot solve the algebraic system resulting from the Helmholtz equation with very high wave number.

## 4. Implementation of the DD algorithm

In this section, we shall derive the preconditioned system of the new DD algorithm and discretize it by finite element method. For simplicity we assume that $\widetilde{\Omega}$ is a bounded domain with homogeneous Dirichlet boundary condition on the upper and bottom boundary and the absorbing boundary condition $\frac{\partial u}{\partial n} - iku = 0$ on the left and right boundary. Other absorbing boundary conditions can be discussed similarly. The Helmholtz equation is as follows:

$$\begin{aligned} -\triangle u - k^2 u &= f \quad \text{in } \widetilde{\Omega}, \\ u &= 0 \quad \text{on } \Gamma_D \\ \frac{\partial u}{\partial n} - iku &= 0 \quad \text{on } \Gamma_R, \end{aligned} \tag{4.1}$$

where $\Gamma_D, \Gamma_R$ are the boundaries with Dirichlet and the absorbing boundary conditions respectively. The subproblems in our DD algorithm can be written as:

$$\begin{aligned} -\triangle u_j^n - k^2 u_j^n &= f_j \quad \text{in } \widetilde{\Omega}_j, \\ \frac{\partial u_j^n}{\partial n_j} + \gamma_j u_j^n &= g_j^n \quad \text{on } \Gamma_{12}, \\ u_j^n &= 0 \quad \text{on } \Gamma_{Dj} \\ \frac{\partial u_j^n}{\partial n} - iku_j^n &= 0 \quad \text{on } \Gamma_{Rj}, \end{aligned}$$

where $j = 1, 2$, $\Gamma_{Dj} = \Gamma_D \cap \partial\widetilde{\Omega}_j, \Gamma_{Rj} = \Gamma_R \cap \partial\widetilde{\Omega}_j$ and $\Gamma_{12}$ is the interface.

Similar as the discussion in Section 2, the discrete variational form of each subproblem is to find $u_{jh}^n \in V_{jh}$ such that

$$\begin{aligned} (\nabla_h u_{jh}^n, \nabla_h v_h)_{\widetilde{\Omega}_j} - k^2 (u_{jh}^n, v_h)_{\widetilde{\Omega}_j} + \gamma_j \langle \Pi u_{jh}^n, \Pi v_h \rangle_{\Gamma_{12}} \\ -ik\langle \Pi u_{jh}^n, \Pi v_h \rangle_{\Gamma_{Rj}} = (f_j, v_h)_{\widetilde{\Omega}_j} + \langle g_j^n, \Pi v_h \rangle_{\Gamma_{12}} \quad \forall v_h \in V_{jh}, \end{aligned} \tag{4.2}$$

where $(\nabla_h u_{jh}^n, \nabla_h v_h)_{\widetilde{\Omega}_j} = \sum_{e \in \tau(\widetilde{\Omega}_j)} (\nabla u_{jh}^n, \nabla v_h)_e, \tau(\widetilde{\Omega}_j)$ is the triangulation of $\widetilde{\Omega}_j$, $V_{jh}$ is the finite element space and the projection operator $\Pi$ shall be defined later.

Let $\tilde{A}_j$ be the stiffness matrix of each problem on subdomain $\widetilde{\Omega}_j$, then $\tilde{A}_j$ can be expressed as

$$\tilde{A}_j = \begin{bmatrix} \tilde{A}_{jII} & \tilde{A}_{jI\Gamma_{12}} \\ \tilde{A}_{j\Gamma_{12}I} & \tilde{A}_{j\Gamma_{12}\Gamma_{12}} \end{bmatrix}, \tag{4.3}$$

where the subscripts $\Gamma_{12}$ and $I$ denote the degrees of freedom on the interface and the other part of the subdomain respectively. By changing the Robin interface condition into Neumann condition or equivalently setting $\gamma_j = 0$ in (4.2), the stiffness matrix $A_j$ is of the form

$$A_j = \begin{bmatrix} A_{jII} & A_{jI\Gamma_{12}} \\ A_{j\Gamma_{12}I} & A_{j\Gamma_{12}\Gamma_{12}} \end{bmatrix}.$$

It is easy to verify that $\tilde{A}_{jII} = A_{jII}, \tilde{A}_{jI\Gamma_{12}} = A_{jI\Gamma_{12}}, \tilde{A}_{j\Gamma_{12}I} = A_{j\Gamma_{12}I}$, $\tilde{A}_{j\Gamma_{12}\Gamma_{12}} = A_{j\Gamma_{12}\Gamma_{12}} + \gamma_j M_{\Gamma_{12}}$, where $M_{\Gamma_{12}}$ is the mass matrix on the interface corresponding to the term $\langle \Pi u_{jh}^n, \Pi v_h \rangle_{\Gamma_{12}}$ in (4.2).

Define $\Pi : V_{jh}|_{\Gamma_{12}} \to M_{jh}$ to be the $L^2$ projection operator such that

$$\langle \Pi u_{jh}, v_h \rangle_{\Gamma_{12}} = \langle u_{jh}, v_h \rangle_{\Gamma_{12}}, \quad \forall v_h \in M_{jh},$$

where $M_{jh}$ is the subspace of $V_{jh}|_{\Gamma_{12}}$. If $V_{jh}$ is $P_1$ conforming finite element space, $M_{jh} = V_{jh}|_{\Gamma_{12}}$ and $\Pi$ is the identify operator in this case; if $V_{jh}$ is Crouzeix–Raviart non-conforming finite element space, $M_{jh}$ is the piecewise constant space, *i.e.* [17],

$$M_{jh} := \{\psi_{jh} : \psi_{jh}|_e \text{ is constant for } \forall e \text{ the element of the triangulation on } \Gamma_{12}\}.$$

A direct observation of the definitions of the space $M_{jh}$ leads to the assertion that $M_{\Gamma_{12}}$ is the tridiagonal matrix and identity matrix $I$ in the cases of $P_1$ conforming and Crouzeix–Raviart non-conforming finite element discretization respectively.

Notice that the stiffness matrix of the problem (4.1) on $\widetilde{\Omega}$ is

$$A = \begin{bmatrix} A_{1II} & 0 & A_{1I\Gamma_{12}} \\ 0 & A_{2II} & A_{2I\Gamma_{12}} \\ A_{1\Gamma_{12}I} & A_{2\Gamma_{12}I} & A_{\Gamma_{12}\Gamma_{12}} \end{bmatrix}.$$

The Schur complement is $S = A_{\Gamma_{12}\Gamma_{12}} - A_{1\Gamma_{12}I}A_{1II}^{-1}A_{1I\Gamma_{12}} - A_{2\Gamma_{12}I}A_{2II}^{-1}A_{2I\Gamma_{12}}$. Obviously, $A_{\Gamma_{12}\Gamma_{12}} = A_{1\Gamma_{12}\Gamma_{12}} + A_{2\Gamma_{12}\Gamma_{12}}$, which leads to $S = S_1 + S_2$, where $S_j = A_{j\Gamma_{12}\Gamma_{12}} - A_{j\Gamma_{12}I}A_{jII}^{-1}A_{jI\Gamma_{12}}$ is the Schur complement corresponding to $A_j$. The discrete Schur complement system of the problem (4.1) on the domain $\widetilde{\Omega}$ is

$$Sw_h = \tilde{f}$$

where $\tilde{f} = \tilde{f}_1 + \tilde{f}_2$ with $\tilde{f}_j = f_{j\Gamma_{12}} - A_{j\Gamma_{12}I}A_{jII}^{-1}f_{jI}$ and $w_h$ is the degrees of freedom on the interface $\Gamma_{12}$ (see [19] for details).

Let $w_{jh}^n$ be the degrees of freedom of $u_{jh}^n$ restricted to $\Gamma_{12}$. Then by the variational form (4.2) and the definition of $\tilde{A}_j$ in (4.3), we have

$$w_{jh}^n = \tilde{S}_j^{-1}(M_{\Gamma_{12}}g_j^n + \tilde{f}_j),$$

where $\tilde{S}_j = \tilde{A}_{j\Gamma_{12}\Gamma_{12}} - \tilde{A}_{j\Gamma_{12}I}\tilde{A}_{jII}^{-1}\tilde{A}_{jI\Gamma_{12}} = \gamma_j M_{\Gamma_{12}} + S_j$. To avoid the computation of the normal derivatives when we update the interface transmission conditions

$$g_2^n = -\frac{\partial u_1^n}{\partial n_1} + \gamma_2 u_1^n \quad \text{and} \quad g_1^* = -\frac{\partial u_2^n}{\partial n_2} + \gamma_1 u_2^n,$$

we use the equivalent form

$$g_2^n = -g_1^n + (\gamma_1 + \gamma_2)u_1^n \quad \text{and} \quad g_1^* = -g_2^n + (\gamma_1 + \gamma_2)u_2^n$$

instead. Finally, the discrete form of the DD iteration procedure can be expressed explicitly as follows:

1. Solve for $w_{1h}^n$ on $\widetilde{\Omega}_1$
$$w_{1h}^n = (\gamma_1 M_{\Gamma_{12}} + S_1)^{-1}(M_{\Gamma_{12}}g_1^n + \tilde{f}_1).$$
2. Update the transmission condition along the interface $\Gamma_{12}$
$$g_2^n = -g_1^n + (\gamma_1 + \gamma_2)\Pi w_{1h}^n.$$
3. Solve for $w_{2h}^n$ on $\widetilde{\Omega}_2$
$$w_{2h}^n = (\gamma_2 M_{\Gamma_{12}} + S_2)^{-1}(M_{\Gamma_{12}}g_2^n + \tilde{f}_2).$$
4. Update the transmission condition along the interface again
$$g_1^* = -g_2^n + (\gamma_1 + \gamma_2)\Pi w_{2h}^n.$$
5. Relax the transmission condition along the interface
$$g_1^{n+1} = \theta g_1^* + (1-\theta)g_1^n.$$

Eliminating the variables $w_{1h}^n, w_{2h}^n, g_2^n, g_1^*$, we get

$$\begin{aligned} g_1^{n+1} = {} & g_1^n + \theta\{(\gamma_1+\gamma_2)[(\gamma_1+\gamma_2)(\gamma_2 M_{\Gamma_{12}} + S_2)^{-1}M_{\Gamma_{12}} - I](\gamma_1 M_{\Gamma_{12}} + S_1)^{-1}\tilde{f}_1 \\ & + (\gamma_1+\gamma_2)(\gamma_2 M_{\Gamma_{12}} + S_2)^{-1}\tilde{f}_2 - (I - [(\gamma_1+\gamma_2)(\gamma_2 M_{\Gamma_{12}} + S_2)^{-1}M_{\Gamma_{12}} - I] \\ & \cdot [(\gamma_1+\gamma_2)(\gamma_1 M_{\Gamma_{12}} + S_1)^{-1}M_{\Gamma_{12}} - I])g_1^n\}. \end{aligned}$$

Then the preconditioned system corresponding to the above iteration method is

$$Pg_1 = f_{g1}, \tag{4.4}$$

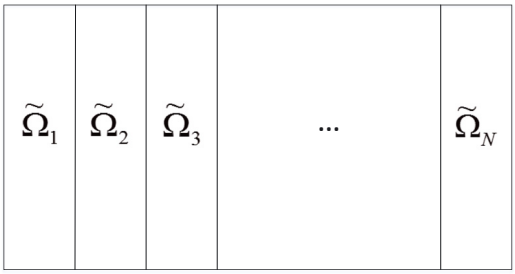


FIGURE 2. The $N$ subdomains partition of $\widetilde{\Omega}$.

where

$$P = I - [(\gamma_1+\gamma_2)(\gamma_2 M_{\Gamma_{12}} + S_2)^{-1} M_{\Gamma_{12}} - I] \cdot [(\gamma_1+\gamma_2)(\gamma_1 M_{\Gamma_{12}} + S_1)^{-1} M_{\Gamma_{12}} - I]$$

and

$$\begin{aligned} f_{g1} = &(\gamma_1+\gamma_2)[(\gamma_1+\gamma_2)(\gamma_2 M_{\Gamma_{12}} + S_2)^{-1} M_{\Gamma_{12}} - I](\gamma_1 M_{\Gamma_{12}} + S_1)^{-1} \tilde{f}_1 \\ &+ (\gamma_1+\gamma_2)(\gamma_2 M_{\Gamma_{12}} + S_2)^{-1} \tilde{f}_2. \end{aligned}$$

The linear system (4.4) may be directly solved by GMRES method and then $u_{1h}^n, u_{2h}^n$ can be computed automatically.

In the case of Crouzeix–Raviart non-conforming finite element discretization, $M_{\Gamma_{12}} = I$ and then

$$\begin{aligned} P &= I - [(\gamma_1+\gamma_2)(\gamma_2 I + S_2)^{-1} - I] \cdot [(\gamma_1+\gamma_2)(\gamma_1 I + S_1)^{-1} - I] \\ &= (\gamma_2 I + S_2)^{-1}[(\gamma_2 I + S_2)(\gamma_1 I + S_1) - (\gamma_1 I - S_2)(\gamma_2 I - S_1)](\gamma_1 I + S_1)^{-1} \\ &= (\gamma_2 I + S_2)^{-1}[(\gamma_1+\gamma_2)(S_1+S_2)](\gamma_1 I + S_1)^{-1} \\ &= (\gamma_1+\gamma_2)(\gamma_2 I + S_2)^{-1} S (\gamma_1 I + S_1)^{-1}. \end{aligned}$$

So $P$ can be viewed as the left and right preconditioning system for the Schur complement $S$.

## 5. Extension to many subdomains case

In this section, we shall extend the above preconditioned system to the many subdomains case. We focus on the problem (4.1). It can also be done in the same way for the case that the absorbing boundary condition is set on the upper and bottom boundary. We split the domain $\widetilde{\Omega}$ into $N$ subdomains in $x$ direction (see Fig. 2). The interfaces are $\Gamma_{jj+1} = \partial\widetilde{\Omega}_j \cap \partial\widetilde{\Omega}_{j+1}, j = 1, 2, \ldots, N-1$. The Dirichlet boundary $\Gamma_{Dj} = \Gamma_D \cap \partial\widetilde{\Omega}_j$. Let $\Gamma_{01} := \Gamma_R \cap \partial\widetilde{\Omega}_1$ and $\Gamma_{NN+1} := \Gamma_R \cap \partial\widetilde{\Omega}_N$. Define $g_{lj}^1, g_{rj}^1$ to be the left boundary conditions of $\widetilde{\Omega}_j$, and $g_{lj}^2, g_{rj}^2$

to be its right boundary conditions, and note that $g_{l1}^{1}=0$, $g_{rN}^{2}=0$. Then the iterative DD algorithm can be defined as follows:

Set $g_{l1}^{1,n}=0$, $g_{rN}^{2,n}=0$. Assume that $g_{lj}^{2,n}$, $g_{rj+1}^{2,n}$, $j=1,2,\ldots,N-1$ is known. As $j$ growing from 1 to $N-1$, we have

1. Solve for $u_{lj}^{n+1/2}$ on $\widetilde{\Omega}_j$

$$\begin{cases} -\triangle u_{lj}^{n+1/2}-k^2u_{lj}^{n+1/2}=f_j & \text{in } \widetilde{\Omega}_j,\\ \dfrac{\partial u_{lj}^{n+1/2}}{\partial n_j}+\gamma_1 u_{lj}^{n+1/2}=g_{lj}^{2,n} & \text{on } \Gamma_{jj+1},\\ u_{lj}^{n+1/2}=0 & \text{on } \Gamma_{Dj},\\ \dfrac{\partial u_{lj}^{n+1/2}}{\partial n_j}-iku_{lj}^{n+1/2}=g_{lj}^{1,n} & \text{on } \Gamma_{j-1j}. \end{cases} \tag{5.1}$$

2. Update the transmission condition along the interface $\Gamma_{jj+1}$

$$g_{rj+1}^{1,n}=-\frac{\partial u_{lj}^{n+1/2}}{\partial n_j}+\gamma_2 u_{lj}^{n+1/2}.$$

3. If $j\neq N-1$, solve for $u_{rj+1}^{n+1/2}$ on $\widetilde{\Omega}_{j+1}$

$$\begin{cases} -\triangle u_{rj+1}^{n+1/2}-k^2u_{rj+1}^{n+1/2}=f_{j+1} & \text{in } \widetilde{\Omega}_{j+1},\\ \dfrac{\partial u_{rj+1}^{n+1/2}}{\partial n_{j+1}}+\gamma_2 u_{rj+1}^{n+1/2}=g_{rj+1}^{1,n} & \text{on } \Gamma_{jj+1},\\ u_{rj+1}^{n+1/2}=0 & \text{on } \Gamma_{Dj+1},\\ \dfrac{\partial u_{rj+1}^{n+1/2}}{\partial n_{j+1}}-iku_{rj+1}^{n+1/2}=g_{rj+1}^{2,n} & \text{on } \Gamma_{j+1j+2}. \end{cases} \tag{5.2}$$

4. If $j\neq N-1$, update the transmission condition along the interface $\Gamma_{jj+1}$

$$g_{lj+1}^{1,n}=\frac{\partial u_{rj+1}^{n+1/2}}{\partial n_{j+1}}-iku_{rj+1}^{n+1/2}.$$

Noticing that $g_{rN}^{2,n+1}=0$, as $j$ decreasing from $N-1$ to 1, we have

5. Solve for $u_{rj+1}^{n+1}$ on $\widetilde{\Omega}_{j+1}$

$$\begin{cases} -\triangle u_{rj+1}^{n+1}-k^2u_{rj+1}^{n+1}=f_{j+1} & \text{in } \widetilde{\Omega}_{j+1},\\ \dfrac{\partial u_{rj+1}^{n+1}}{\partial n_{j+1}}+\gamma_2 u_{rj+1}^{n+1}=g_{rj+1}^{1,n} & \text{on } \Gamma_{jj+1},\\ u_{rj+1}^{n+1}=0 & \text{on } \Gamma_{Dj+1},\\ \dfrac{\partial u_{rj+1}^{n+1}}{\partial n_{j+1}}-iku_{rj+1}^{n+1}=g_{rj+1}^{2,n+1} & \text{on } \Gamma_{j+1j+2}. \end{cases} \tag{5.3}$$

6. Update the transmission condition along the interface $\Gamma_{jj+1}$

$$\begin{aligned} g_{lj}^{2,n+1/2}&=-\frac{\partial u_{rj+1}^{n+1}}{\partial n_{j+1}}+\gamma_1 u_{rj+1}^{n+1},\\ g_{lj}^{2,n+1}&=\theta g_{lj}^{2,n+1/2}+(1-\theta)g_{lj}^{2,n}. \end{aligned}$$

7. If $j \neq 1$, solve for $u_{lj}^{n+1}$ on $\widetilde{\Omega}_j$

$$\begin{cases} -\triangle u_{lj}^{n+1} - k^2 u_{lj}^{n+1} = f_j & \text{in } \widetilde{\Omega}_j, \\ \dfrac{\partial u_{lj}^{n+1}}{\partial n_j} + \gamma_1 u_{lj}^{n+1} = g_{lj}^{2,n+1} & \text{on } \Gamma_{jj+1}, \\ u_{lj}^{n+1} = 0 & \text{on } \Gamma_{Dj}, \\ \dfrac{\partial u_{lj}^{n+1}}{\partial n_j} - iku_{lj}^{n+1} = g_{lj}^{1,n} & \text{on } \Gamma_{j-1j}. \end{cases} \tag{5.4}$$

8. If $j \neq 1$, update the transmission condition along the interface $\Gamma_{jj+1}$

$$g_{rj}^{2,n+1/2} = \frac{\partial u_{rj}^{n+1}}{\partial n_j} - iku_{rj}^{n+1},$$
$$g_{rj}^{2,n+1} = \theta g_{rj}^{2,n+1/2} + (1-\theta) g_{rj}^{2,n}.$$

This algorithm is a sweeping procedure. In practical computation, we do not use the above iterative DD algorithm directly. Actually we shall look for a preconditioner from above DD algorithm, then use PGMRES to solve the preconditioned system.

Let $V_{jh}$ be the finite element space in each subdomain $\widetilde{\Omega}_j$. Then the above discrete variational form in each subdomain is to find $u_{ljh} \in V_{jh}$ such that

$$\begin{aligned} (\nabla_h u_{ljh}, \nabla_h v_h)_{\widetilde{\Omega}_j} - k^2 (u_{ljh}, v_h)_{\widetilde{\Omega}_j} + \gamma_1 \langle \Pi u_{ljh}, \Pi v_h \rangle_{\Gamma_{jj+1}} - ik \langle \Pi u_{ljh}, \Pi v_h \rangle_{\Gamma_{j-1j}} \\ = (f_j, v_h)_{\widetilde{\Omega}_j} + \langle g_{lj}^2, \Pi v_h \rangle_{\Gamma_{jj+1}} + \langle g_{lj}^1, \Pi v_h \rangle_{\Gamma_{j-1j}} \quad \forall v_h \in V_{jh}, \end{aligned} \tag{5.5}$$

and to find $u_{rjh} \in V_{jh}$ such that

$$\begin{aligned} (\nabla_h u_{rjh}, \nabla_h v_h)_{\widetilde{\Omega}_j} - k^2 (u_{rjh}, v_h)_{\widetilde{\Omega}_j} + \gamma_2 \langle \Pi u_{rjh}, \Pi v_h \rangle_{\Gamma_{j-1j}} - ik \langle \Pi u_{rjh}, \Pi v_h \rangle_{\Gamma_{jj+1}} \\ = (f_j, v_h)_{\widetilde{\Omega}_j} + \langle g_{rj}^1, \Pi v_h \rangle_{\Gamma_{j-1j}} + \langle g_{rj}^2, \Pi v_h \rangle_{\Gamma_{jj+1}} \quad \forall v_h \in V_{jh}. \end{aligned} \tag{5.6}$$

Let $A_{lj}$, $A_{rj}$ be the stiffness matrices associated with (5.5), (5.6) respectively. Define the restriction matrices $T_j^1, T_j^2$ to be that $T_j^1 u_{jh} = \Pi(u_{jh}|_{\Gamma_{j-1j}})$ and $T_j^2 u_{jh} = \Pi(u_{jh}|_{\Gamma_{jj+1}})$ for $\forall u_{jh} \in V_{jh}$ respectively. The corresponding prolongation matrices can be defined as the transposes of $T_j^1, T_j^2$, *i.e.*, $P_j^1 := (T_j^1)^T$ and $P_j^2 := (T_j^2)^T$. Let $M_{\Gamma_{jj+1}}$ be the mass matrix which is related to the term $\langle \Pi u_{jh}, \Pi v_h \rangle_{\Gamma_{jj+1}}$ on the interface $\Gamma_{jj+1}$ for $\forall j = 0, \ldots, N$. The matrix form for the subdomain can be expressed as:

$$A_{lj} u_{ljh} = f_j + P_j^1 M_{\Gamma_{j-1j}} g_{lj}^1 + P_j^2 M_{\Gamma_{jj+1}} g_{lj}^2, \tag{5.7}$$

where $j = 1, \ldots, N-1$. Similarly, we have

$$A_{rj} u_{rjh} = f_j + P_j^1 M_{\Gamma_{j-1j}} g_{rj}^1 + P_j^2 M_{\Gamma_{jj+1}} g_{rj}^2, \tag{5.8}$$

where $j = 2, \ldots, N$. Now we further define

$$
\begin{aligned}
A^{1,1}_{lj,rj} &:= -I + (\gamma_2 + ik)T^1_j A^{-1}_{rj} P^1_j M_{\Gamma_{j-1j}},\\
A^{1,1}_{rj,lj-1} &:= -(\gamma_1 + \gamma_2)T^2_{j-1} A^{-1}_{lj-1} P^1_{j-1} M_{\Gamma_{j-2j-1}},\\
A^{1,2}_{lj,rj} &:= (\gamma_2 + ik)T^1_j A^{-1}_{rj} P^2_j M_{\Gamma_{jj+1}},\\
A^{1,2}_{rj,lj-1} &:= I - (\gamma_1 + \gamma_2)T^2_{j-1} A^{-1}_{lj-1} P^2_{j-1} M_{\Gamma_{j-1j}},\\
A^{2,1}_{lj,rj+1} &:= I - (\gamma_1 + \gamma_2)T^1_{j+1} A^{-1}_{rj+1} P^1_{j+1} M_{\Gamma_{jj+1}},\\
A^{2,1}_{rj,lj} &:= (\gamma_1 + ik)T^2_j A^{-1}_{lj} P^1_j M_{\Gamma_{j-1j}},\\
A^{2,2}_{lj,rj+1} &:= -(\gamma_1 + \gamma_2)T^1_{j+1} A^{-1}_{rj+1} P^2_{j+1} M_{\Gamma_{j+1j+2}},\\
A^{2,2}_{rj,lj} &:= -I + (\gamma_1 + ik)T^2_j A^{-1}_{lj} P^2_j M_{\Gamma_{jj+1}},\\
f^1_{lj} &:= -(\gamma_2 + ik)T^1_j A^{-1}_{rj} f_j,\\
f^1_{rj} &:= (\gamma_1 + \gamma_2)T^2_{j-1} A^{-1}_{lj-1} f_{j-1},\\
f^2_{lj} &:= (\gamma_1 + \gamma_2)T^1_{j+1} A^{-1}_{rj+1} f_{j+1},\\
f^2_{rj} &:= -(\gamma_1 + ik)T^2_j A^{-1}_{lj} f_j,
\end{aligned}
$$

where $I$ is the identity matrix. Define matrices $A_{11}, A_{12}, A_{21}, A_{22}$ as follows:

$$
A_{11} = \begin{pmatrix}
I & & & & & \\
A^{1,1}_{l2,r2} & I & & & & \\
 & A^{1,1}_{r3,l2} & I & & & \\
 & & & \ddots & & \\
 & & & A^{1,1}_{lN-1,rN-1} & I & \\
 & & & & A^{1,1}_{rN,lN-1} & I
\end{pmatrix},
$$

$$
A_{12} = \begin{pmatrix}
 & & & & & A^{1,2}_{r2,l1} \\
 & & & & A^{1,2}_{l2,r2} & \\
 & & & A^{1,2}_{r3,l2} & & \\
 & & \iddots & & & \\
 & A^{1,2}_{lN-1,rN-1} & & & & \\
A^{1,2}_{rN,lN-1} & & & & &
\end{pmatrix},
$$

$$
A_{21} = \begin{pmatrix}
 & & & & & A^{2,1}_{lN-1,rN} \\
 & & & & A^{2,1}_{rN-1,lN-1} & \\
 & & & A^{2,1}_{lN-2,rN-1} & & \\
 & & \iddots & & & \\
 & A^{2,1}_{r2,l2} & & & & \\
A^{2,1}_{l1,r2} & & & & &
\end{pmatrix},
$$

and

$$A_{22} = \begin{pmatrix} I & & & & & \\ A^{2,2}_{rN-1,lN-1} & I & & & & \\ & A^{2,2}_{lN-2,rN-1} & I & & & \\ & & & \ddots & & \\ & & & A^{2,2}_{r2,l2} & I & \\ & & & & A^{2,2}_{l1,r2} & I \end{pmatrix}.$$

Let

$$g_1 = (g^1_{r2} \quad g^1_{l2} \dots g^1_{lN-1} \quad g^1_{rN})^T, g_2 = (g^2_{lN-1} \quad g^2_{rN-1} \dots g^2_{r2} \quad g^2_{l1})^T,$$
$$f_1 = (f^1_{r2} \quad f^1_{l2} \dots f^1_{lN-1} \quad f^1_{rN})^T, f_2 = (f^2_{lN-1} \quad f^2_{rN-1} \dots f^2_{r2} \quad f^2_{l1})^T.$$

Let $\widetilde{A}_{21} = \theta A_{21}$, $\widetilde{A}_{22} = \theta A_{22}$, $\widetilde{A}_{22(1)} = (1-\theta)I + \widetilde{A}_{22}$, and $\widetilde{f}_2 = \theta f_2$. By simple manipulation, we obtain the preconditioned system

$$\widetilde{A}^{-1}_{22(1)}(\widetilde{A}_{22} - \widetilde{A}_{21}A^{-1}_{11}A_{12})g_2 = \widetilde{A}^{-1}_{22(1)}(\widetilde{f}_2 - \widetilde{A}_{21}A^{-1}_{11}f_1), \tag{5.9}$$

which is corresponding to the iterative DD procedure. Here the parameter is chosen to be $\theta = \frac{1}{2}$, which is the same as the two subdomains case. Note that $N = 2$, system (5.9) reduces to the system (4.4), so (5.9) is a reasonable extension of the two subdomains case.

The next theorem shows that the system (5.9) is equivalent to the global problem, and we may use the GMRES method to solve it.

**Theorem 5.1.** *For the algebraic system* (5.9)*, there exists a unique solution, which is equivalent to the solution of the original global problem.*

*Proof.* For starting the proof, we first need to know the well-definedness of the matrices and vectors in (5.9), which depend on the existence of matrices $A^{-1}_{lj}$ and $A^{-1}_{rj}$. According to the above discussion, $A^{-1}_{lj}$ and $A^{-1}_{rj}$ correspond to solving subproblems (5.1), (5.4) and (5.2), (5.3) respectively. In fact, we already know in Section 2 that there exist unique solutions to these subproblems (see [15] for details) and then $A_{lj}$ and $A_{rj}$ are invertible. Meanwhile, $A_{11}$ is also invertible in (5.9) since $A_{11}$ is a lower triangular matrix with identity matrices in its block diagonal. Similarly, $\widetilde{A}_{22(1)}$ is invertible.

We then prove the equivalence. Obviously, (5.9) is equivalent to the coupled algebraic system

$$\begin{bmatrix} A_{11} & A_{12} \\ A_{21} & A_{22} \end{bmatrix} \begin{bmatrix} g_1 \\ g_2 \end{bmatrix} = \begin{bmatrix} f_1 \\ f_2 \end{bmatrix}, \tag{5.10}$$

which actually is the same as system

$$g^2_{lj} = (\gamma_1 + \gamma_2)T^1_{j+1}u_{rj+1h} - g^1_{rj+1}, \qquad j = 1, \dots, N-1 \tag{5.11}$$
$$g^1_{lj} = -(\gamma_2 + ik)T^1_j u_{rjh} + g^1_{rj}, \qquad j = 2, \dots, N-1 \tag{5.12}$$
$$g^1_{rj} = (\gamma_1 + \gamma_2)T^2_{j-1}u_{lj-1h} - g^2_{lj-1}, \qquad j = 2, \dots, N \tag{5.13}$$
$$g^2_{rj} = -(\gamma_1 + ik)T^2_j u_{ljh} + g^2_{lj}, \qquad j = 2, \dots, N-1 \tag{5.14}$$

together with subproblems (5.7) and (5.8).

By (5.11) and (5.13), we know that $T^2_j u_{ljh} = T^1_{j+1}u_{rj+1h}$ for $j = 1, \dots, N-1$. Denote $A_{jI}$ to be the stiffness matrix in $\widetilde{\Omega}_j$ with Neumann boundary condition on $\Gamma_{j-1j}$ and $\Gamma_{jj+1}$. Then, the matrices $A_{lj}, A_{rj}$ can be expressed as

$$A_{lj} = A_{jI} - ikP^1_j M_{\Gamma_{j-1j}}T^1_j + \gamma_1 P^2_j M_{\Gamma_{jj+1}}T^2_j, \tag{5.15}$$
$$A_{rj} = A_{jI} + \gamma_2 P^1_j M_{\Gamma_{j-1j}}T^1_j - ikP^2_j M_{\Gamma_{jj+1}}T^2_j. \tag{5.16}$$

By (5.7), (5.8), (5.12), and (5.14), we have

$$\begin{aligned} A_{lj}u_{ljh} - A_{rj}u_{rjh} &= (P_j^1 M_{\Gamma_{j-1j}} g_{lj}^1 + P_j^2 M_{\Gamma_{jj+1}} g_{lj}^2) - (P_j^1 M_{\Gamma_{j-1j}} g_{rj}^1 + P_j^2 M_{\Gamma_{jj+1}} g_{rj}^2) \\ &= -(\gamma_2 + ik) P_j^1 M_{\Gamma_{j-1j}} T_j^1 u_{rjh} + (\gamma_1 + ik) P_j^2 M_{\Gamma_{jj+1}} T_j^2 u_{ljh}. \end{aligned}$$

Substituting (5.15), (5.16) into the above equation, then we get

$$(A_{jI} - ikP_j^1 M_{\Gamma_{j-1j}} T_j^1 - ikP_j^2 M_{\Gamma_{jj+1}} T_j^2) u_{ljh} = (A_{jI} - ikP_j^1 M_{\Gamma_{j-1j}} T_j^1 - ikP_j^2 M_{\Gamma_{jj+1}} T_j^2) u_{rjh},$$

which is equivalent to $u_{ljh} = u_{rjh}$ by the invertibility of matrix $A_{jI} - ikP_j^1 M_{\Gamma_{j-1j}} T_j^1 - ikP_j^2 M_{\Gamma_{jj+1}} T_j^2$. Let $u_h \in V_h$, where $V_h$ is the finite element space in the whole domain $\widetilde{\Omega}$, which obviously satisfy that $u_h|_{\widetilde{\Omega}_j} = u_{rjh}, j = 2, \ldots, N$ and $u_h|_{\widetilde{\Omega}_1} = u_{l1h}$. Define the restriction matrix $T_j$ to be that $T_j v_h = (v_h|_{\widetilde{\Omega}_j}), \forall v_h \in V_h$, and the corresponding prolongation matrix $P_j := T_j^T$. Obviously, $T_j^2 T_j = T_{j+1}^1 T_{j+1}$ and $P_j P_j^2 = P_{j+1} P_{j+1}^1$. Then we have

$$\begin{aligned} &P_1 A_{l1} u_{l1h} + \sum_{j=2}^{N} P_j A_{rj} u_{rjh} \\ &= \sum_{j=1}^{N} P_j A_{jI} T_j u_h - ikP_1 P_1^1 M_{\Gamma_{01}} T_1^1 T_1 u_h - ikP_N P_N^2 M_{\Gamma_{NN+1}} T_N^2 T_N u_h \\ &- ik \sum_{j=2}^{N-1} P_j P_j^2 M_{\Gamma_{jj+1}} T_j^2 T_j u_h + \gamma_1 P_1 P_1^2 M_{\Gamma_{12}} T_1^2 T_1 u_h + \gamma_2 \sum_{j=2}^{N} P_j P_j^1 M_{\Gamma_{j-1j}} T_j^1 T_j u_h \\ &= \sum_{j=1}^{N} P_j f_j + P_1 P_1^1 M_{\Gamma_{01}} g_{l1}^1 + P_N P_N^2 M_{\Gamma_{NN+1}} g_{rN}^2 \\ &+ P_1 P_1^2 M_{\Gamma_{12}} g_{l1}^2 + \sum_{j=2}^{N} P_j P_j^1 M_{\Gamma_{j-1j}} g_{rj}^1 + \sum_{j=2}^{N-1} P_j P_j^2 M_{\Gamma_{jj+1}} g_{rj}^2. \end{aligned}$$

By (5.11), (5.14) and simple manipulation, it is easy to verify that

$$\begin{aligned} -ik \sum_{j=2}^{N-1} P_j P_j^2 M_{\Gamma_{jj+1}} T_j^2 T_j u_h + \gamma_1 P_1 P_1^2 M_{\Gamma_{12}} T_1^2 T_1 u_h + \gamma_2 \sum_{j=2}^{N} P_j P_j^1 M_{\Gamma_{j-1j}} T_j^1 T_j u_h \\ = P_1 P_1^2 M_{\Gamma_{12}} g_{l1}^2 + \sum_{j=2}^{N} P_j P_j^1 M_{\Gamma_{j-1j}} g_{rj}^1 + \sum_{j=2}^{N-1} P_j P_j^2 M_{\Gamma_{jj+1}} g_{rj}^2, \end{aligned}$$

which leads to

$$\begin{aligned} \sum_{j=1}^{N} P_j A_{jI} T_j u_h - ikP_1 P_1^1 M_{\Gamma_{01}} T_1^1 T_1 u_h - ikP_N P_N^2 M_{\Gamma_{NN+1}} T_N^2 T_N u_h \\ = \sum_{j=1}^{N} P_j f_j + P_1 P_1^1 M_{\Gamma_{01}} g_{l1}^1 + P_N P_N^2 M_{\Gamma_{NN+1}} g_{rN}^2. \end{aligned}$$

So $u_h$ is the unique solution of (4.1), and then we finish the proof. □

TABLE 1. The iteration numbers for different methods and different mesh sizes. The wave number $k = 9.5\pi$.

| $h$ | RO | OS | T-OS |
|---|---|---|---|
| $\frac{1}{60}$ | 6 | 386 | 251 |
| $\frac{1}{120}$ | 7 | 235 | 126 |
| $\frac{1}{240}$ | 7 | 288 | 132 |
| $\frac{1}{480}$ | 7 | 393 | 153 |
| $\frac{1}{960}$ | 7 | >500 | 182 |

TABLE 2. The iteration numbers of PGMRES for different methods and different mesh sizes. The wave number $k = 9.5\pi$.

| $h$ | RO | OS | T-OS | FETI-H |
|---|---|---|---|---|
| $\frac{1}{60}$ | 5 | 15 | 13 | 20 |
| $\frac{1}{120}$ | 5 | 19 | 16 | 28 |
| $\frac{1}{240}$ | 4 | 23 | 17 | 36 |
| $\frac{1}{480}$ | 4 | 29 | 18 | 46 |
| $\frac{1}{960}$ | 4 | 36 | 21 | 58 |

## 6. NUMERICAL RESULTS

In this section, we shall give some numerical results to illustrate the efficiency of our new DD method. Consider the following Helmholtz equation

$$\begin{aligned} -\triangle u - k^2 u &= f \quad \text{in } \Omega, \\ \frac{\partial u}{\partial n} - iku &= 0 \quad \text{on } \Gamma_R, \\ u &= 0 \quad \text{on } \Gamma_D, \end{aligned} \tag{6.1}$$

where $\Omega$ is the unit square $[0,1] \times [0,1]$, $\Gamma_R$ denotes $x = 0$ and $x = 1$, which is the Robin boundary condition, and $\Gamma_D$ is the boundary $y = 0$ and $y = 1$ with homogeneous Dirichlet boundary condition. The source term $f = exp\{-h^{-2}[(x-1/2)^2 + (y-1/2)^2]\}$ is a gaussian function which is an approximation of the point source $(\frac{1}{2}, \frac{1}{2})$ with exponential decay off the center. Here we choose the Crouzeix−Raviart non-conforming finite element to discretize this model problem. $P_1$ conforming finite element has similar performance behavior. Our iterative procedure is proposed for the continuous case, however for the discrete case the pollution error can not be avoidable for the uniform mesh [1]. Because the degrees of freedoms of Crouzeix−Raviart finite element is nearly 3 times as $P_1$ conforming finite element, it may reduce the influence of pollution.

We consider the iteration of our method with different mesh sizes. The parameter chooses $\theta = \frac{1}{2}$ in our iterative method. The iteration stops when $\frac{\|u_{iter} - u_d\|_{l^2}}{\|u_d\|_{l^2}} \leqslant 10^{-10}$, where $u_{iter}$ is the iteration solution, and $u_d$ is the discrete solution. The choices of the Robin transmission condition parameters are $\gamma_1 = \frac{1}{100}k^{1/2}(1-i), \gamma_2 = h^{-2}(1-i)$. We first test our algorithm (RO) with different mesh size for fixed $k$ and compare it to Optimized Schwarz (OS) [13], Two-sided Optimized Schwarz (T-OS) [12] methods. Table 1 shows the corresponding iteration numbers when the mesh is refined.

If these DD methods are used as preconditioners in GMRES iterations, the iteration number greatly decrease. We also compare them to the FETI-H method with coarse space constituted by 4 different direction plan waves in the preconditioned form. The terminal precision of the PGMRES iteration is $10^{-10}$. It can be seen from Table 1 and 2 that our method is better than optimized Schwarz, two-sided optimized Schwarz method and

TABLE 3. The iteration numbers of PGMRES for different methods and different mesh sizes. The wave number $k = 30\pi$.

| $h$ | RO | OS | T-OS | FETI-H |
|---|---|---|---|---|
| $\frac{1}{188}$ | 5 | 21 | 17 | 42 |
| $\frac{1}{376}$ | 4 | 24 | 18 | 51 |
| $\frac{1}{752}$ | 5 | 33 | 22 | 63 |
| $\frac{1}{1504}$ | 5 | 38 | 25 | 80 |

TABLE 4. The iteration numbers of PGMRES with different wave number $k$ and different methods for $kh =$ constant, where $kh \approx 0.5$.

| $k$ | RO | OS | T-OS | FETI-H |
|---|---|---|---|---|
| $9.5\pi$ | 5 | 15 | 15 | 20 |
| $19.5\pi$ | 5 | 18 | 19 | 32 |
| $29.5\pi$ | 4 | 18 | 19 | 38 |
| $39.5\pi$ | 4 | 20 | 21 | 45 |
| $59.5\pi$ | 5 | 25 | 23 | 56 |
| $89.5\pi$ | 5 | 29 | 27 | 65 |
| $100.5\pi$ | 5 | 30 | 28 | 70 |
| $150.5\pi$ | 5 | 35 | 32 | 82 |

TABLE 5. The iteration numbers for different choices of the relaxation parameter $\theta$.

| $\theta$ | 0.1 | 0.2 | 0.3 | 0.4 | 0.5 | 0.6 | 0.7 | 0.8 | 0.9 | 1 |
|---|---|---|---|---|---|---|---|---|---|---|
| $k = 19.5\pi$ | 90 | 40 | 23 | 14 | 7 | 12 | 21 | 35 | 73 | >500 |
| $k = 59.5\pi$ | 78 | 35 | 20 | 12 | 5 | 12 | 20 | 35 | 77 | >500 |

the FETI-H method in this case. Note that the numbers of iteration for $h = 1/60$ in Table 1 is quite large, one reasonable explanation is that the discrete wave number $\widetilde{k}$ is shifted close to the relevant frequency of the whole domain and thus the convergence rate is close to 1 for this mesh parameter. However, this phenomenon disappeared by refining the mesh and $\widetilde{k}$ is close to $k$. Similar phenomenon is also observed in [12, 13].

Now, for a larger $k$, let the frequency $k = 30\pi$, which is a frequency that the the convergence rate may equal 1 in the iterative procedure. So we only focus on the PGMRES iteration. We find that our DD method is still better than other DD methods.

Next, we fix $kh =$ constant to test how the iteration numbers depend on the wave number $k$. We also do this test by PGMRES. It can be seen from Table 4 that the number of iterations of our method is stable as $k$ becomes larger and larger and the iteration numbers are great less than the OS, T-OS and FETI-H methods.

Now we consider how the different choices of the parameters in our method influence the iteration number. The convergence rate sensitively depend on the choice of the relaxation parameter $\theta$ in the iterative method, which is shown in Table 5. We can see that the parameter $\theta = \frac{1}{2}$ which we choose in our numerical test is close to the optimal one. For the Robin parameters, the left graph of Figure 3 shows the iteration numbers for some fixed parameters $\gamma_2$ and different choices of $\gamma_1$. We note that in the left graph, the iteration numbers are almost the same when $C_1 \leqslant \frac{1}{32}$ and $\gamma_1 = C_1 k^{1/2}(1-i)$ for any fixed $\gamma_2$, and the best choice of $\gamma_2$ is $\gamma_2 = h^{-2}(1-i)$ with the least iteration number. So our choice of $\gamma_1 = \frac{1}{100}k^{1/2}(1-i)$ in the previous numerical tests is suitable. The right graph of Figure 3 shows the iteration numbers for some fixed parameters $\gamma_1$ and different choices of $\gamma_2$.

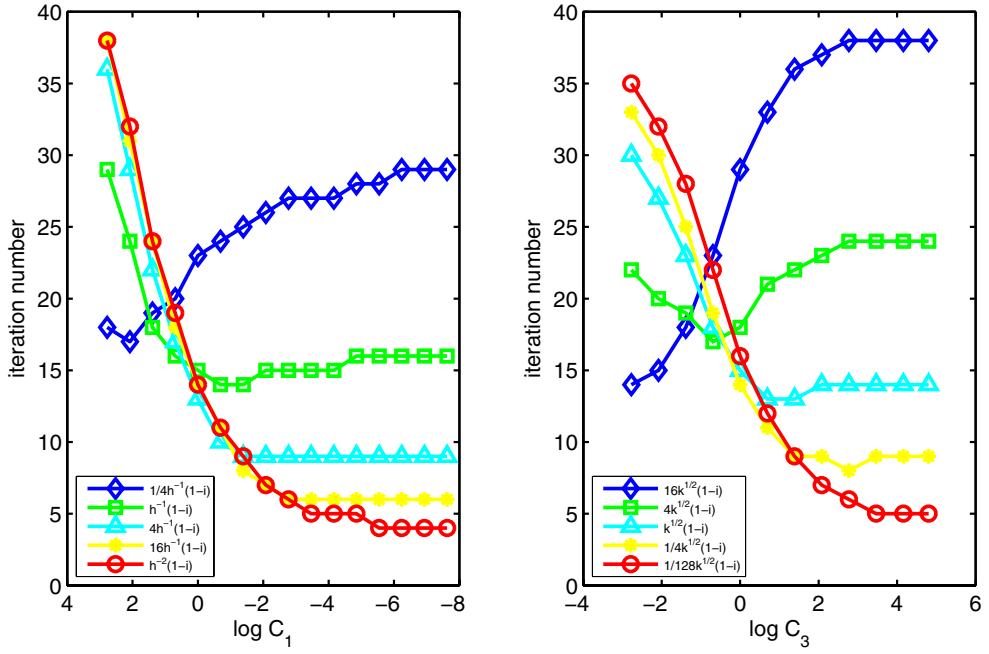


FIGURE 3. The iteration numbers of PGMRES for different choices of the Robin parameters. The wave number is $k = 19.5\pi$, and the mesh size is $h = 0.0082$, which implies $kh = 0.5023$. *Left:* the iteration numbers with $\gamma_2 = 1/4h^{-1}(1-i), h^{-1}(1-i), 4h^{-1}(1-i), 16h^{-1}(1-i), h^{-2}(1-i)$ over $\gamma_1 = C_1 k^{1/2}(1-i)$, where $C_1 = 2^s, s = 4, 3, \ldots, -11$. *Right:* the iteration numbers with $\gamma_1 = 16k^{1/2}(1-i), 4k^{1/2}(1-i), k^{1/2}(1-i), 1/4k^{1/2}(1-i), 1/128k^{1/2}(1-i)$ over $\gamma_2 = C_3 h^{-1}(1-i)$, where $C_3 = 2^t, t = -4, -3, \ldots, 6$ and $C_3 = h^{-1}$.

Similarly, we observe that the iteration numbers are almost the same when $C_3 \geqslant 16$ and $\gamma_2 = C_3 h^{-1}(1-i)$ for any fixed $\gamma_1$, and the choice $\gamma_1 = \frac{1}{128}k^{1/2}(1-i)$ performs best with the least iteration number. Note that $h = 0.0082$ and $h^{-2} \approx 122h^{-1}$, the optimal choice that $\gamma_2 = h^{-2}(1-i)$ is better than $\gamma_2 = C_3 h^{-1}(1-i)$ with $C_3 \leqslant 16$, and this phenomena is consistent with the observation in Remark 3.7. The discussion above also implies that our choices of the Robin parameters do not affect the optimality of our DD method.

We further consider the following model problem

$$\begin{aligned} -\triangle u - k^2 u &= f \quad \text{in } \Omega, \\ \frac{\partial u}{\partial n} - iku &= 0 \quad \text{on } \Gamma, \end{aligned} \tag{6.2}$$

where $\Gamma$ is the boundary of $\Omega$ with Robin boundary condition and the source term $f$ is the same as problem (6.1). This type problems are widely used in practical computation. We only test the iteration number of PGMRES for this problem. The result (see Tab. 6) also shows that our method is stable and better than the other three DD methods. If the domain is divided by $x = \frac{1}{3}$ instead of $x = \frac{1}{2}$, and the source term $f = \exp\{-h^{-2}[(x - 1/3)^2 + (y - 1/2)^2]\}$, then we will have a similar result in Table 7.

Next, we shall consider two kinds of more complicated domains. Let $\Omega_d$ to be a diamond domain with the four vertices $(\frac{1}{2}, 0), (0, \frac{1}{2}), (1, \frac{1}{2}), (\frac{1}{2}, 1)$ (see the left graph of Fig. 4). The corresponding equation can be written as

$$\begin{aligned} -\triangle u - k^2 u &= f \quad \text{in } \Omega_d, \\ \frac{\partial u}{\partial n} - iku &= 0 \quad \text{on } \Gamma, \end{aligned} \tag{6.3}$$

TABLE 6. The iteration numbers of different wave number $k$ and different methods for $kh =$ constant, where $kh \approx 0.5$.

| $k$ | RO | OS | T-OS | FETI-H |
|---|---|---|---|---|
| $10\pi$ | 5 | 13 | 14 | 22 |
| $20\pi$ | 4 | 15 | 16 | 30 |
| $40\pi$ | 4 | 17 | 18 | 43 |
| $80\pi$ | 4 | 19 | 20 | 56 |
| $160\pi$ | 4 | 21 | 22 | 68 |

TABLE 7. The iteration numbers of different wave number $k$ and different methods for non-symmetric decomposition with $kh =$ constant, where $kh \approx 0.5$.

| $k$ | RO | OS | T-OS | FETI-H |
|---|---|---|---|---|
| $10\pi$ | 6 | 14 | 14 | 24 |
| $20\pi$ | 7 | 15 | 16 | 34 |
| $40\pi$ | 8 | 17 | 18 | 46 |
| $80\pi$ | 8 | 19 | 20 | 57 |
| $160\pi$ | 9 | 21 | 22 | 70 |

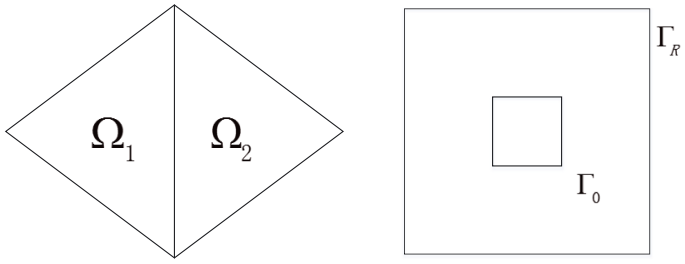


FIGURE 4. Left: the diamond domain. Right: the domain with a scatterer.

TABLE 8. The iteration numbers of different wave number $k$ and different methods with $kh =$ constant, where $kh \approx 0.5$ (domain $\Omega_d$).

| $k$ | RO | OS | T-OS |
|---|---|---|---|
| $10\pi$ | 4 | 13 | 14 |
| $20\pi$ | 4 | 15 | 16 |
| $40\pi$ | 4 | 17 | 18 |
| $80\pi$ | 4 | 19 | 20 |
| $160\pi$ | 4 | 21 | 22 |

where $\Gamma$ is the boundary of $\Omega_d$ with Robin boundary condition and the source term $f$ is the same as problem (6.1). The result in Table 8 reveals that our method is also stable and superior to other two DD methods. Next, let $\Omega_o$ to be a domain $[0,1] \times [0,1]$ without inner part $[\frac{2}{5}, \frac{3}{5}] \times [\frac{2}{5}, \frac{3}{5}]$ (see the right graph of Fig. 4).

TABLE 9. The iteration numbers of different wave number $k$ and different methods with $kh =$ constant, where $kh \approx 0.5$ (domain $\Omega_o$).

| $k$ | RO | OS | T-OS |
|---|---|---|---|
| $10\pi$ | 6 | 16 | 16 |
| $20\pi$ | 7 | 17 | 17 |
| $40\pi$ | 8 | 18 | 19 |
| $80\pi$ | 8 | 19 | 21 |
| $160\pi$ | 9 | 21 | 23 |

TABLE 10. The iteration numbers of different wave number $k$ and different methods for $kh =$ constant with 2nd order absorbing boundary condition, where $kh \approx 0.5$.

| $k$ | RO | OS | T-OS | FETI-H |
|---|---|---|---|---|
| $10\pi$ | 4 | 11 | 12 | 20 |
| $20\pi$ | 4 | 14 | 10 | 31 |
| $40\pi$ | 4 | 16 | 12 | 44 |
| $80\pi$ | 4 | 18 | 14 | 57 |
| $160\pi$ | 4 | 23 | 17 | 73 |

TABLE 11. The iteration numbers of different wave number $k$ and different number of subdomains $N$, for $kh =$ constant, where $kh \approx 0.5$, $\theta = 1/2$.

| $k$ | RO | | | FETI-H | | |
|---|---|---|---|---|---|---|
| | $N = 4 \times 1$ | $N = 8 \times 1$ | $N = 16 \times 1$ | $N = 2 \times 2$ | $N = 3 \times 3$ | $N = 4 \times 4$ |
| 16 | 10 | 15 | 22 | 12 | 18 | 16 |
| 32 | 11 | 16 | 22 | 20 | 42 | 34 |
| 64 | 11 | 15 | 22 | 31 | 86 | 74 |
| 128 | 11 | 16 | 23 | 46 | 190 | 215 |
| 256 | 11 | 16 | 23 | 62 | 442 | >500 |
| 512 | 11 | 16 | 23 | 81 | >500 | >500 |
| 1024 | 11 | 16 | 23 | 100 | >500 | >500 |

Then the equation is as follows:

$$\begin{aligned} -\triangle u - k^2 u &= f_1 \quad \text{in } \Omega_o, \\ \frac{\partial u}{\partial n} &= 0 \quad \text{on } \Gamma_0, \\ \frac{\partial u}{\partial n} - iku &= 0 \quad \text{on } \Gamma_R, \end{aligned} \tag{6.4}$$

where $\Gamma_0$ is the internal boundary, $\Gamma_R$ is the external boundary and the source term is $f_1 = exp\{-h^{-2}[(x - 1/2)^2 + (y-1)^2]\}$. In this case, we also find that our method is better than the other two DD methods in Table 9. Note that we always use the lowest order absorbing boundary condition $\frac{\partial u}{\partial n} - iku = 0$ in the above numerical tests. Actually, our method may still work for higher order boundary condition according to our theory. For the problem (6.1), if we use 2nd order absorbing boundary condition $\frac{\partial u}{\partial n} - iku - \frac{i}{2k}\frac{\partial^2 u}{\partial \tau^2} = 0$ on $\Gamma_R$, where $\tau$ denotes the tangent direction at the boundary, we have the result shown in Table 10, which indicates that our new DD method is still stable and outperform the other three DD methods.

For many subdomains case, we consider the problem (6.2). Because of the suitable choice of the parameters, we also find that the iteration number of the new system (5.9) is independent of $k$ (see Tab. 11 for details) and $h$

TABLE 12. The iteration numbers of different mesh size $h$ and different number of subdomains $N$, $\theta = 1/2$. The wave number $k = 64$.

| $h$ | RO | | | FETI-H | | |
|---|---|---|---|---|---|---|
| | $N = 4 \times 1$ | $N = 8 \times 1$ | $N = 16 \times 1$ | $N = 2 \times 2$ | $N = 3 \times 3$ | $N = 4 \times 4$ |
| $\frac{1}{128}$ | 11 | 15 | 22 | 31 | 86 | 74 |
| $\frac{1}{256}$ | 11 | 15 | 22 | 43 | 94 | 86 |
| $\frac{1}{512}$ | 11 | 15 | 22 | 59 | 104 | 104 |
| $\frac{1}{1024}$ | 11 | 15 | 22 | 80 | 117 | 134 |

(see Tab. 12 for details). However it may increase as the number of subdomains increasing, which may be due to the lack of the coarse space. For the other optimized Schwarz methods, the iteration number also increases as the number of the subdomains becomes large. Similar situation also happens for the FETI-H, FETI-DPH or BDDC-H methods. But we believe that the iteration number may keep stable if the the coarse space is sufficiently large.

## 7. Conclusion

A new and robust two parameters Robin−Robin nonoverlapping domain decomposition method for the Helmholtz problems is introduced in this paper. We analyze the convergence rate of this method for a model problem with two subdomains case by Fourier transform. It is proved that by suitable choice of parameters, the convergence rate $\rho < 1$ is independent of the mesh size for fixed $k$ and the wave number for $kh =$ constant. We also extend this method to the many subdomains case. Numerical experiments further show that the DD method holds optimal convergence rate.

*Acknowledgements.* We thank the anonymous referees who made many helpful comments and suggestions which lead to an improved presentation of this paper.

## References

[1] I.M. Babuška and S.A. Sauter, Is the pollution effect of the FEM avoidable for the Helmholtz equation considering high wave numbers? *SIAM Rev.* **42** (2000) 451–484.

[2] A. Brandt and I. Livshits, Wave-ray multigrid method for standing wave equations, *Electron. Trans. Numer. Anal.* **6** (1997) 162–181.

[3] W. Chen, X. Xu and S. Zhang, On a Robin−Robin domain decomposition method with optimal convergence rate. *J. Comput. Math.* **32** (2014) 456–475.

[4] Q. Deng, A nonoverlapping domain decomposition method for nonconforming finite element problems. *Commun. Pure Appl. Anal.* **2** (2003) 295–306.

[5] B. Despres, Domain Decomposition Method and Helmholtz Problem. Mathematical and Numerical Aspects of Wave Propagation Phenomena, edited by G. Cohen, L. Halpern and P. Joly. Philadelphia, SIAM (1991) 44–52.

[6] J. Douglas and C.S. Huang, An accelerated domain decomposition procedures based on Robin transmission conditions. *BIT* **37** (1997) 678-686.

[7] J. Douglas and C.S. Huang, Accelerated domain decomposition iterative procedures for mixed methods based on Robin transmission conditions. *Calcolo* **35** (1998) 131–147.

[8] O.G. Ernst and M.J. Gander, Why is Difficult to Solve Helmholtz Problems with Classical Iterative Methods. Numerical Analysis of Multiscale Problems, edited by I. Graham, T. Hou, O. Lakkis and R. Scheichl. Springer-Verlag, New York (2011) 325–363.

[9] C. Farhat, A. Macedo and R. Tezaur, FETI-H: A Scalable Domain Decomposition Method for High Frequency Exterior Helmholtz Problem. In 11th International Conference on Domain Decomposition Method, edited by P. Bjørstad, M. Cross and O. Widlund. Choi-Hong Lai, DDM.ORG (1999) 231–241.

[10] C. Farhat, P. Avery, R. Tezaur and J. Li, FETI-DPH: a dual-primal domain decomposition method for accoustic scattering. *J. Comput. Acoustics* **13** (2005) 499–524.

[11] M.J. Gander, L. Halpern and F. Nataf, Optimized Schwarz Methods. In 12th International Conference on Domain Decomposition Methods, edited by T. Chan, T. Kako, H. Kawarada and O. Pironneau. Chiba, Japan, Domain Decomposition Press (2001) 15–18.

[12] M.J. Gander, L. Halpern and F. Magoules, An optimized Schwarz method with two-sided Robin transmission conditions for the Helmholtz equation. *Int. J. Numer. Meth. Fluids* **55** (2007) 163–175.

[13] M.J. Gander, F. Magoules and F. Nataf, Optimized Schwarz methods without overlap for the Helmholtz equation. *SIAM J. Sci. Comput.* **24** (2002) 38–60.

[14] W. Guo and L.S. Hou, Generalization and accelerations of Lions' nonoverlapping domain decomposition method for linear elliptic PDE. *SIAM J. Numer. Anal.* **41** (2003) 2056–2080.

[15] F. Ihlenburg, Finite Element Analysis of Acoustic Scattering. Vol. 132 of *Appl. Math. Sci.* Springer-Verlag, New York (1998).

[16] J. Li and X. Tu, Convergence analysis of a balancing domain decomposition method for solving a class of indefinite linear systems. *Numer. Linear Algebra Appl.* **16** (2009) 745–773.

[17] L. Qin and X. Xu, On a parallel Robin-type nonoverlapping domain decomposition method. *SIAM J. Numer. Anal.* **44** (2006) 2539–2558.

[18] L. Qin, Z. Shi and X. Xu, On the convergence rate of a parallel nonoverlapping domain decomposition method. *Sci. China, Ser. A: Math.* **51** (2008) 1461–1478.

[19] A. Toselli and O. Widlund, Domain Decomposition Methods-Algorithms and Theory. Vol. 34 of *Springer Ser. Comput. Math.* Springer-Verlag, Berlin (2005).

[20] M.B. Van Gijzen, Y.A. Erlangga and C. Vuik, Spectral analysis of the discrete Helmholtz operator preconditioned with a shifted Laplacian. *SIAM J. Sci. Comput.* **29** (2007) 1942–1958.

[21] X. Xu and L. Qin, Spectral analysis of DN operators and optimized Schwarz methods with Robin transmission conditions. *SIAM J. Numer. Anal.* **47** (2010) 4540–4568.